Available online at www.sciencedirect.com
ScienceDirect
Journal of Molecular Catalysis B: Enzymatic 48 (2007) 90–98
JOURNAL OF MOLECULAR CATALYSIS B: ENZYMATIC
www.elsevier.com/locate/molcatb

Immobilization of chloroperoxidase on silica-based materials for 4,6-dimethyl dibenzothiophene oxidation

Carmina Montiel, Eduardo Terrés, José-Manuel Domínguez, Jorge Aburto *

Instituto Mexicano del Petróleo, Eje Central Lázaro Cárdenas 152, 07730 Mexico City, Mexico

Received 3 January 2007; received in revised form 26 June 2007; accepted 29 June 2007
Available online 10 July 2007

Abstract

Silica-based materials have been used as effective supports for the immobilization of enzymes. Moreover, the understanding on the oxidation of sulfur compounds by immobilized chloroperoxidase represents a step further in the development of a biocatalytic desulfurization process of fossil fuels. Here, chloroperoxidase from *Caldariomyces fumago* was immobilized on amorphous and structured silica-based materials either physically or covalently using an organosilane derivative for the oxidation of a recalcitrant organosulfur compound currently found in gas oil and diesel, such as 4,6-dimethyldibenzothiophene (4,6-DMDBT). Such materials were characterized by FTIR, N_2-adsorption, XRD, SEM and TEM. We have found that the chemical differences on the silanol/siloxane groups of SG/67 and SBA15 mesoporous materials deeply modify the enzymatic load, activity, thermal stability and reusability. The physical immobilization of CPO was characterized by a high adsorption capacity (q_m) and affinity constants (K_m) when compared to the covalent approach, but it resulted more sensitive to temperature than free, the silanized and covalently immobilized enzyme. The thermal residual activity as well as reusability of CPO were first improved by silanization, then by covalent immobilization in a support with a large pore size and high silanol/siloxane ratio.

Keywords: Chloroperoxidase; Immobilization; Mesoporous materials; Desulfurization; 4,6-Dimethyldibenzothiophene

1. Introduction

Silica-based materials have been extensively studied in various fields of chemistry and material science in the last years with a special attraction to bioapplications such as antibacterial agents [1], biosensors [2] supports or adsorbents [3,4]. These materials include porous glass [5], sol–gel [6] and more recently mesoporous materials [4,5]. The latter are inorganic hosts obtained by self-assembling of organic surfactants under an hydrothermal treatment with variable pore size, different array symmetry and particular pore structures [6]. Their high surface area (up to 1500 $m^2\ g^{-1}$) and pore size (up to 300 Å) render them ideal materials for supporting chemical species or for several adsorbents applications [3]. Such versatility permits the design of tailored supports with different chemical pore environments for binding of ligands through physical or covalent interactions [7]. Besides, the adsorption of catalytic proteins (enzymes) into mesoporous materials is a relatively young research area where the main studies have been addressed to increase the enzyme stability or to facilitate the biocatalyst recovery and recycling as well as their utilization in harsh media.

Among the known mesoporous materials, SBA15 is a good candidate as enzyme support because of its uniform pores up to 300 Å, thick pore walls and high hydrothermal stability [8]. A variety of proteins like cytochrome *C* (Cyt *C*), conalbumin, lysozyme, and myoglobin have been immobilized on functionalized SBA15 with high enzymatic loads and activities with not diffusional limitations [9,10]. For example, it has been suggested that the high activity of immobilized Cyt *C* on SBA15 might come from the protein interaction with the surface of the mesoporous material. Here, the Fe(III) ion changes between the low to high spin from the soluble to the immobilized protein [2]. Furthermore, immobilized Cyt *C* was stable under denaturing conditions and remained active for several months [11].

Chloroperoxidase (CPO) from *Caldariomyces fumago* (E.C. 1.11.1.10) is a very interesting enzyme because of the diverse kind of reactions promoted by, i.e. sulfoxidation [12,13],

* Corresponding author. Tel.: +52 55 9175 8204; fax: +52 55 9175 8429.
E-mail address: jaburto@imp.mx (J. Aburto).

1381-1177/$ – see front matter © 2007 Elsevier B.V. All rights reserved.
doi:10.1016/j.molcatb.2007.06.012

epoxidation [12], oxidation of alcohols to aldehydes [14], hydrogen peroxide dismutation [15,16] and halogenation reactions [17]. CPO immobilization has been studied by physical adsorption on talc [18], celite [19] and mesoporous materials such as MCM48, SBA15 and SBA16 [20,21]. Besides, CPO has been also attached by covalent binding in polyurethane [22], aminopropyl-glass [23] and SBA16 [21]. These studies employed small molecules as substrates like monochlorodimedone (MCD) or thioanisole to study the catalytic activity of immobilized CPO against pH, temperature or denaturing agents. Nevertheless, none of such studies was focused on the biocatalytic behavior on an organic solvent/aqueous media to resolve an industrial concern such as sulfur content in fuels.

The oil refining industry represents one of the potential uses of CPO in the production of clean fuels such as gas oil, diesel and gasoline in order to meet the present rigorous environmental regulations [24]. Indeed, CPO catalyzes the oxidization of the sulfur-containing compounds present in fuels such as 4,6-dimethyldibenzothiophene (4,6-DMDBT) [25]. For example, Vazquez-Duhalt et al. [24] proposed the biocatalytic oxidation and subsequent separation of organosulfur compounds by distillation to obtain low-sulfur fuels. However, the technological and economical feasibility of such biocatalytic process presents an important shortcoming, the low operational stability of CPO in organic media.

In order to contribute to the knowledge of the biocatalytic production of clean fuels, CPO was immobilized in this work through physical and tailored-covalent adsorption on silica gel (amorphous) and SBA15 with two different pore sizes (ordered materials). The main purpose was to ascertain the effect of the immobilization approach and material type on the oxidization of a recalcitrant organosulfur compound commonly found in gas oil and diesel, i.e. 4,6-DMDBT. The silica-based materials were previously well characterized by N_2-adsorption isotherms, XRD, FTIR, SEM, and TEM. The adsorption isotherms of CPO on silica-based materials were characterized and their effectiveness in the oxidation of 4,6-DMDBT was evaluated in terms of kinetic parameters, thermal residual activity and reusability.

2. Experimental

2.1. Materials

3-Aminopropyl triethoxysilane (APTES), 1-[3-(dimethylamino)propyl]-3-ethyl carbodiimide hydrochloride, hydrogen peroxide, and 4,6-dimethyl dibenzothiophene (4,6-DMDBT) were purchased from Sigma Chemical Co. Tetraethylorthosilicate (TEOS, 98%), silica gel (SG/67, 67 Å pore size, surface area ~500 $m^2\ g^{-1}$), succinic anhydride and the triblock copolymer poly(ethylene oxide)–poly(propylene oxide)–poly(ethylene oxide) (Pluronic P123, mw 5800, $EO_{20}PO_{70}EO_{20}$) were obtained from Aldrich Co. Buffer salts were purchased from J.T. Baker. Chloroperoxidase from *C. fumago* (42 kDa, Rz = 1.4) was kindly provided by Dr. Michael A. Pickard from the University of Alberta in Canada.

2.2. Synthesis of SBA15

The parent SBA15 material was synthesized using Pluronic P123 as a structure-directing agent according to the method reported in the literature [8]. Here, 4 g of Pluronic P123 were dissolved in 105 mL of water with HCl 37% (20 mL) and the solution was stirred for a few hours. Then, 9 g of tetraethylorthosilicate were added and the resulting solution was first heated at 40 °C for 24 h and subsequently heated at 100 °C for another 24 h under stirring. The parent SBA15 material was obtained under vacuum at 40 °C while the material with a 67 Å pore size (SBA15/67) was obtained by calcination in the presence of air at 550 °C.

In order to increase the pore diameter of SBA15, the alcothermal method was performed. Here, 1 g of P123 was dissolved under magnetic stirring in 100 mL of water, then 40 mL of ethanol and 0.1 mL of ammonium hydroxide (5N) were added to the mixture and stirred for 10 min at room temperature. Afterwards, 1 g of the parent SBA15 material was added to the solution and heated at 100 °C for 96 h in order to obtain a 143 Å pore size. The drying and calcination processes were carried out as described above and the material was referred hereafter as SBA15/143.

2.3. Characterization of the silica-based materials

All silica-based materials were characterized before and after enzyme immobilization by N_2-adsorption, XRD and FTIR. The adsorption–desorption isotherms were obtained at 77 K with an automatic volumetric sorption analyzer Micromeritics ASAP-2000 using N_2 as sorbent. In a typical experiment, the material was outgassed at 240 °C for 3 h prior to the adsorption measurements. In the case of enzyme-loaded materials, they were out gassed at 30 °C for 24 h to prevent the thermal denaturation of the enzyme. The surface area was determined from the BET equation, while the mean pore size was obtained from the pore size distribution using the desorption isotherm branch data and the Barret–Joyner–Halenda (BJH) method. X-ray diffraction patterns were recorded on a Siemens D500 (λ_{Cu} = 1.54 Å) between 0.5° and 10° (2Θ). The FTIR spectra were acquired by diffuse reflectance using KBr as the dispersing phase using a 470 Nicolet Avatar FTIR spectrometer. Moreover, SBA15/67 and SBA15/143 were studied by TEM and SEM using a high-resolution transmission electron microscope FEI Tecnai F30 (300 kV) and a Phillips XL30 ESEM scanning electron microscope, respectively.

2.4. Covalent modification of chloroperoxidase with APTEOSB

APTEOSB was used as a covalent spacer arm between the silica-based materials and CPO and synthesized as reported elsewhere [21] using an equimolar concentration of 3-aminopropyl triethoxysilane and succinic anhydride, which reacted over night under nitrogen atmosphere at room temperature.

Twenty-four milligrams of APTEOSB and 11 mg of carbodiimide were dissolved in 3 mL of phosphate buffer (pH 5,

60 mM) followed by CPO addition to obtain an APTEOSB/CPO molar ratio of 1500:1. The reaction was performed during 2 h at 4 °C and the resulting solution was dialyzed during 24 h in phosphate buffer (1 L, pH 5.0) to eliminate the unreactive reagents. The silanized-CPO is further referred as s-E.

The CPO modification was detected by steady state fluorescence spectroscopy using a RF-5301 PC Shimadzu Spectrofluorometer, with a 150 W Xe lamp at 25 °C. The emission spectra were measured with an excitation wavelength of 290 nm in order to measure the contribution of the tryptophan groups in the fluorescence emission.

2.5. Immobilization of chloroperoxidase

A solution of free CPO (18 μM) dissolved in acetate buffer (60 mM, pH 3) was added to 100 mg of every silica-based material (SBA15/67, SBA15/143 or SG/67) to proceed to physical CPO adsorption. Besides, a solution of s-E (18 μM) dissolved in phosphate buffer (60 mM, pH 5) was added to 100 mg of every silica-based material for the covalent immobilization of CPO and referred hereafter using the material designation plus the suffix s-E. Enzyme loading on every material was accomplished by orbital agitation during 4 h at 4 °C. Then, the materials were separately recovered by centrifugation and washed three-time (3× 1 mL) with their respective aqueous buffer. The amount of immobilized enzyme on every silica-based material was calculated by subtracting the amount recovered in the supernatant liquid from the initial amount of enzyme, using an extinction coefficient of 85,000 M^{-1} cm^{-1} at the Soret band (398 nm). Before use, all immobilized CPO materials were maintained during 48 h over a saturated solution of $CaCl_2$ to equilibrate the humidity (31%). The adsorption isotherms of CPO were collected after 16 h at 4 °C using an enzymatic concentration between 0 and 18 μM.

2.6. Enzymatic activity

For the evaluation of the enzymatic activity, the oxidative reaction of 4,6-DMDBT was performed. In a typical experiment, 10 mg of immobilized CPO, acetate buffer (60 mM, pH 3), a KCl solution (20 mM) and an acetonitrile solution of 4,6-DMDBT (7 μM) were added to a 3-mL quartz cell in order to obtain an acetonitrile content of 20% (v/v). The reaction was started by the addition of an aliquot of H_2O_2 to reach a cell concentration of 0.25 mM under magnetic agitation and followed by fluorometry during 2 min at 25 °C (λ_{exc} 240 and λ_{ems} 346 nm). The 4,6-DMDBT oxidation was determined using a pre-elaborated calibration curve. Besides, kinetic curves were obtained between 1 and 8 μM of 4,6-DMDBT and each initial velocity was calculated from less than 10% of substrate oxidation in order to be in rapid equilibrium condition. The data were fitted to the Hill equation according to previously own work [25]. The chemical oxidation of 4,6-DMDBT induced by H_2O_2 was negligible under the conditions studied here. Every assay was repeated at least three times to assure reproducibility.

2.7. Thermal residual activity and reusability of CPO-immobilized materials

The stability of the enzymatic preparations in terms of residual activity was evaluated as a function of temperature from 25 to 50 °C. Free, silanized and immobilized enzymes were separately incubated at a specific temperature during 2 h. Then, the residual enzymatic activity was determined at 25 °C for 4,6-DMDBT oxidation as described above. All the residual activity data were normalized to the assays at 25 °C, which was considered as 100% activity.

Moreover, the reusability of all prepared biocatalysts were assayed in five sequential cycles for the oxidation of 4,6-DMDBT in the miscible acetonitrile/buffer media (20:80%, v/v) as mentioned earlier. The immobilized CPO was recovered by centrifugation at 14,000 rpm during 1 min among reaction cycles and poured in a fresh reaction media. The residual activity data were normalized to the first cycle assay of every tested biocatalyst, which was considered as 100% activity.

3. Results and discussion

3.1. Characterization of silica-based materials

The X-ray diffraction (XRD) pattern of the parent material (SBA15/67, Fig. 1a) showed three well-resolved peaks with distances of 93.9, 54.5 and 47.4 Å, that correspond to (1 0 0), (1 1 0) and (2 0 0) reflections. The latter indexed to a hexagonal structure with lattice constant of 107.8 Å ($a_0 = 2d(1\,0\,0)/\sqrt{3}$), which is typical for a SBA15 pore structure as reported elsewhere [8]. Compared with SBA15/67, the silica gel did not show any array at small angle (data not shown), which is a characteristic of an amorphous material. The XRD pattern of SBA15/143 could not be obtained because of instrumental limitations to work at lower angles than 0.5 (2Θ).

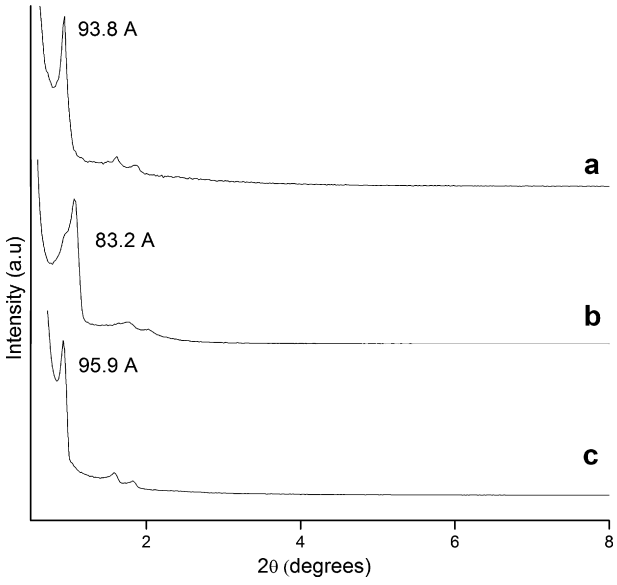

Fig. 1. X-ray diffraction pattern of SBA15/67 (a), after CPO physical loading on SBA15/67 (b), and after CPO covalent immobilization, SBA15/67-s-E (c).

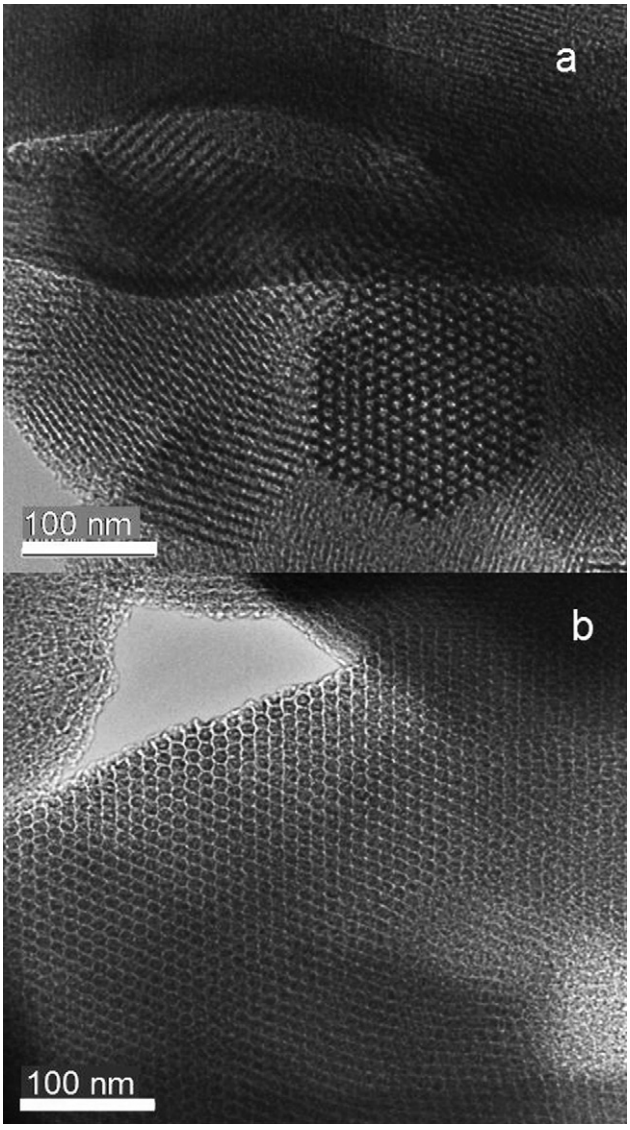

Fig. 2. Micrographs of SBA15 mesoporous materials with a main pore size of 67 Å (a) and 143 Å (b) obtained by TEM.

In the case of SBA15/67 after physical CPO adsorption, the material showed a displacement of the (1 0 0) reflection from 93.8 to 83.2, which revealed a certain contraction of its structure (Fig. 1b). These changes can be explained by the acidic conditions (pH 3) imposed to the material during the enzyme immobilization. On the other hand, the SBA15/67-s-E structure was not affected by the milder basic conditions (pH 5) during the covalent immobilization of CPO (Fig. 1c). Nevertheless, the hexagonal structure of SBA15/67 is preserved as suggested by the TEM (Fig. 2a and b) and SEM images (data not shown). It is clear from the photographs that the alcothermal treatment incremented the pore size of SBA15/143.

We determined both the surface area and main pore diameter for SBA15/67, SBA15/143 and SG/67 before and after CPO loading through the N_2 adsorption isotherms (Table 1 and supplementary information). The isotherms are characteristic of a monolayer adsorption followed by capillary condensation at $P/P_0 = 0.73$, 0.92 and 0.74, respectively. They are typical of type IV isotherms, indicating that samples are porous materials according to the IUPAC classification [26]. Moreover, the sharp increase in the adsorption volume around 0.5–0.9 is indicative of the presence of mesopores for the two SBA15 materials.

The SBA materials presented a main pore diameter of 67.1 and 142.5 Å, whilst SG/67 presented a wider pore size distribution with a lower pore volume due to its amorphous nature in contrast to the SBA15 materials (Table 1 and supplementary information). The physical adsorption of CPO in SBA15/67 and SG/67 did not significantly change the main pore size, which remained around 64 Å. Nonetheless, the surface area of CPO-loaded SBA/67 incremented 22% (Table 1) due to contraction of the structure as observed by the XRD pattern. In the case of SBA15/143, the pore size decreased from 143 to 107.7 Å with a light increment in surface area (5%) because of the thicker pore walls that stabilized the material [27]. The maintenance of the pore size in SBA15/67 and SG/67 suggests that CPO molecules should mainly occupy the external surface of the particles while the partial reduction of the pore size in SBA15/143 was attributed to CPO immobilization on the pore mouths.

In regard to covalent immobilization, SG/67 did not suffer any significant change in its textural properties suggesting that CPO immobilization occurred on material's surface. In the case of SBA15/67 and SBA15/143, the pore size decreased to 47.6 and 112.6 Å, respectively; while the surface area decreased about 20% (Table 1). It is evident that the grafting of s-E to the external surface of both SBA15 materials resulted in the partial blockage of pores as earlier described for the grafting of vinyl groups on MCM-41 [28].

3.2. Physical and covalent immobilization of CPO

CPO was readily immobilized in silica-based materials through two essential different methods: (1) adsorption by surface interactions and (2) covalently bonded with APTEOSB as spacer arm. The FTIR spectra of all biocatalytic materials showed the characteristic signals at 3410 and 1640 cm^{-1} due to the bands of amide A and I, respectively, and attributable to the presence of adsorbed CPO (Fig. 3).

The silanized CPO (s-E) showed a blue shift (hypsochromic) in its emission fluorescence spectrum due to a more hydrophobic microenvironment around its triptophan residues (Fig. 4). Besides, the presence of s-E grafted on silica-based materials was identified by deconvolution of the corresponding FTIR spectrum (Fig. 5) using Omnic 5.1 software, FTIR (cm^{-1}): 3629 (νNH), 3398 (νSi–OH), 2977 (νCH_2), 1766 (νCO), 1641 (νCO Amide I band), 1531 (δNH Amide II band), and 1083 (νSiO).

A different strategy consistent on the modification of silica-based materials with APTEOSB followed by CPO grafting resulted in materials with negligible oxidation activity that was possibly due to enzyme deactivation or blockage of its active site (data not shown).

The materials bearing a 67 Å main pore size physically adsorbed more CPO than their covalent counterparts (Table 1). Only the SBA15 bearing a 143 Å main pore adsorbed slightly more CPO through the covalent approach than the physical one. Here, SBA15/67 presented a higher initial surface area that

Table 1
Surface properties of immobilized CPO on silica-based materials

Immobilized enzyme preparation	Main pore diameter (Å)		Surface area ($m^2\ g^{-1}$)		CPO load ($nmol_{CPO}\ g^{-1}$)	Adsorption parameters	
						q_m ($nmol_{CPO}\ g^{-1}$)	K_m (μM^{-1})
SG/67	48–64[a]	48–64[b]	466[a]	473[b]	84.38	1966 ± 170	0.021 ± 0.01
SG/67-s-E	48–64	48–64	466	463	41.5	58.51 ± 5.2	0.215 ± 0.08
SBA15/67	67.1	64.1	715.68	878.37	150.5	622.59 ± 38.73	0.246 ± 0.09
SBA15/67-s-E	67.1	47.6	715.68	569.67	68.5	332.45 ± 59.81	0.093 ± 0.02
SBA15/143	142.5	107.7	380.7	400	157.8	5725 ± 365	0.038 ± 0.01
SBA15/143-s-E	142.5	112.6	380.7	328	172.24	250 ± 35.47	0.061 ± 0.03

[a] Before enzyme immobilization.
[b] After enzyme immobilization.

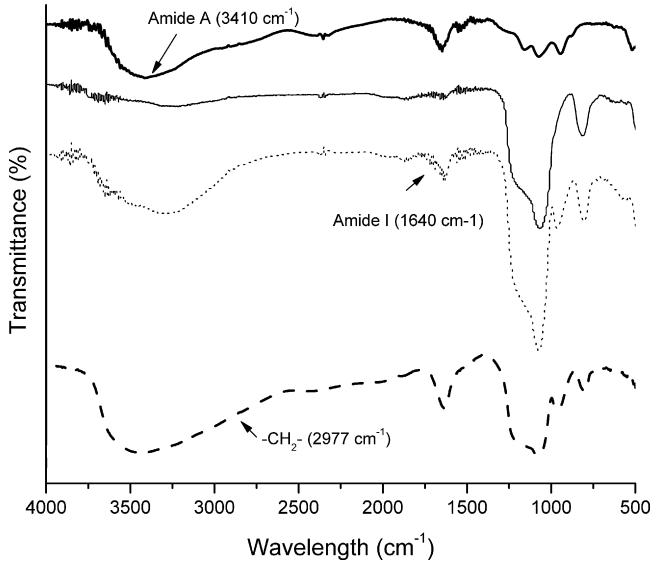

Fig. 3. FTIR spectra of chloroperoxidase (top, bold solid line), SBA15/67 (solid line), CPO adsorbed on SBA15/67 (dashed line), and silanized CPO covalently immobilized on SBA15/67 (SBA15/67-s-E, bold dashed line).

improved enzyme immobilization through physical adsorption, e.g. the SBA15/67 had 1.54 times more surface area than SG/67 which closely corresponds to the respective enzyme loads. It is worth to note that SG/67 presented the lower content of free silanol groups as seen by the FTIR spectra that corresponded to the lower CPO load (Table 1 and supplementary information). Indeed, the area ratio of free silanol to siloxane groups (SiOH/SiO) obtained from FTIR spectra showed a value of 1.0766, 1.3693 and 2.9248 for SG67, SBA15/67 and SBA15/143, respectively. Since the isoelectric point (p*I*) of CPO is ∼4.0, the overall net charge of the protein is slightly positive and such of the silica-based materials is negative (p*I* of $SiO_2 \sim 2$) at pH 3.0. Then, the physical immobilization of CPO on silica-based materials at pH 3.0 should occur through electrostatic interactions because of the correlation between the enzymatic load and the content of free silanol groups on silica-based materials.

Furthermore, the covalent load of CPO on silica-based materials was enhanced by using a larger main pore size and by a higher content of free silanol groups on silica-based materials that could react with the ethoxy silane groups of s-E. It is well known that the silylation reaction uses mainly the silanol

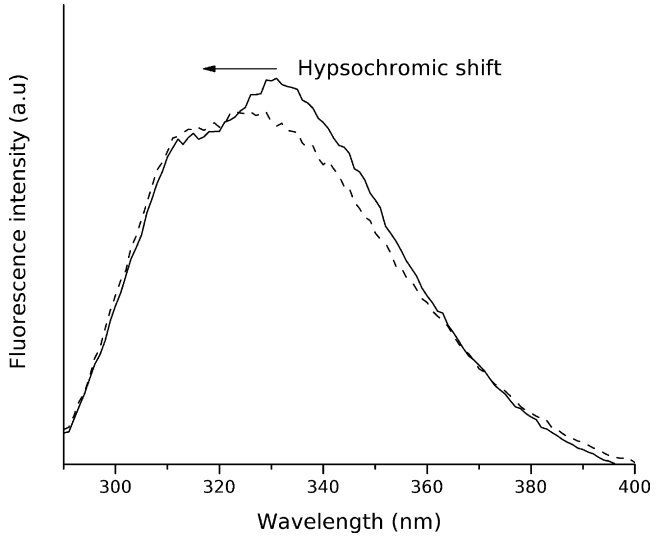

Fig. 4. Changes on the fluorescence spectra of free (solid line) and silanized CPO (dashed line) at 25 °C.

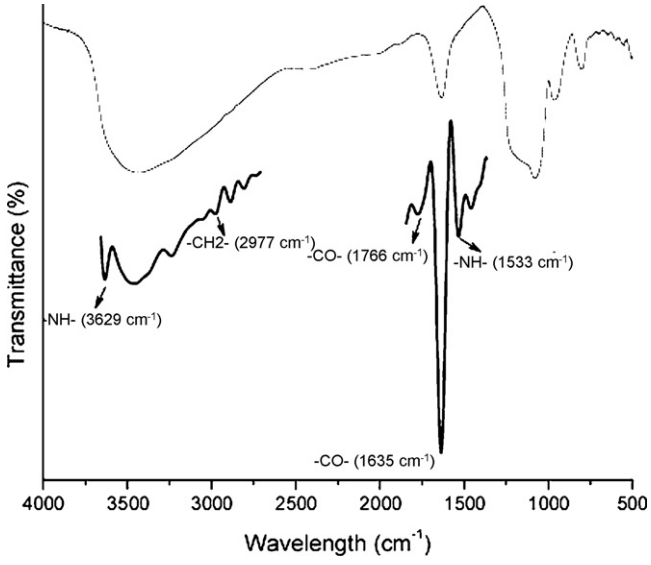

Fig. 5. FTIR spectrum of silanized-CPO covalently immobilized on SBA15 (SBA15/67-s-E, solid line) and its deconvoluted spectrum (bold solid line).

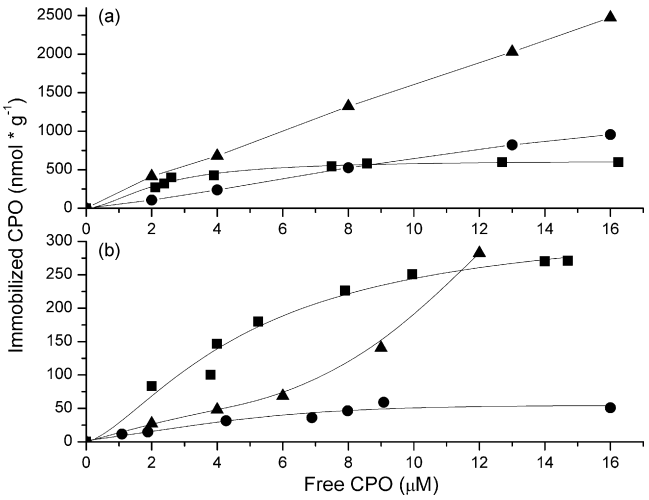

Fig. 6. Adsorption isotherms of CPO at 4 °C by (a) physical immobilization and (b) covalent immobilization on SG/67 (●), SBA15/67 (■), and SBA15/143 (▲).

groups present in the material's surface through single (≡SiOH) and geminal hydroxyl groups (=SiOH), and less with hydrogen bonded silanol groups [29]. Here, it is important to note that covalent immobilization was carried out at pH 5.0 where both materials and CPO present an overall negative charge. Then, the physical immobilization was avoided here as reported by previous works [20,21]. The SBA15/143-s-E bearing the larger pore size loaded 4.2 and 2.5 times more CPO than SG/67-s-E and SBA15/67-s-E, respectively (Table 1). The CPO molecule is an elongated object with long and short axes of ca. 60 and 46 Å, which can access into the mesopore [21]. The reduction in surface area and pore size for SBA15/143-s-E was attributed to the CPO adsorption inside the mesopores or in the vicinity of pore mouths.

Since the immobilization approach could alter the enzyme activity and stability, we considered then important to obtain the adsorption isotherms of CPO in SG/67, SBA15/67 and SBA15/143 through physical and covalent immobilization at 4 °C. All isotherms presented a type I isotherm which is associated with a monolayer adsorption of CPO and known as Langmuir isotherm (Fig. 6). The experimental data were fitted to the Langmuir equation (1) with a correlation value greater than 0.96 (R^2) using Origin 7.0 software in order to determine the monolayer adsorption capacity (q_m) and the Langmuir affinity constant (K_m):

$$q_e = \frac{q_m K_m C_e}{1 + K_m C_e} \quad (1)$$

where q_e is the amount of adsorbed CPO in silica-based materials at equilibrium while C_e is the equilibrium concentration of CPO in the aqueous media [30].

The largest physical adsorption capacity of CPO was observed for SBA15/143 followed by SG/67 and SBA15/67 (Table 1). Here, the larger pore size in SBA15/143 undoubtedly enhanced CPO physical adsorption as discussed above. In the other hand, the minor adsorption capacity for the 67 Å pore size materials was attributed to the smaller pore size and lower silanol/siloxane ratio.

The covalent-bonded CPO to silica-based materials showed also monolayer adsorption isotherms but with reduced binding capacities when compared to physical adsorption (K_m, see Table 1). This is not surprising since covalent bond formation requires more energy that non-covalent interactions while all adsorption isotherms were performed at 4 °C. Moreover, the SBA15 materials presented a higher binding capacity for s-E than SG/67, which corresponded with a higher content of the free silanol groups. Besides, the highest adsorption affinity of CPO was observed for SBA15/143 and SBA15/143-s-E. This was attributed to the major presence of silanol groups for physical or covalent immobilization as well as a larger pore size that undoubtedly favored the CPO affinity of the silica-based materials.

3.3. Oxidation of 4,6-DMDBT by free and immobilized CPO

All CPO preparations (soluble and immobilized) were able to oxidize 4,6-DMDBT to its corresponding sulfone at different extent as seen by the kinetic parameters (Table 2). CPO adsorbed on SG/67, SBA15/67 and SBA15/143 showed a close catalytic turnover (k_{cat}) value of 64.76, 73.4 and 77.82 min^{-1}, respectively. Such catalytic turnover values barely represent the 10–15% of the free enzyme (522.97 min^{-1}) and soluble s-E (638.17 min^{-1}). The increase in the catalytic efficiency of s-E may be due to a change in protein conformation through the chemical modification as seen by fluorometry (Fig. 4), that enhanced the catalytic turnover but not the Hill constant (K_h).

Table 2
Catalytic parameters fitted to the Hill equation of immobilized CPO on silica-based materials

Immobilized enzyme preparation	Kinetic parameters				
	k_{cat} (min^{-1})	K_h (μM)	k_{cat}/K_h ($\mu M^{-1}\,min^{-1}$)	n	R^2
SG/67	64.76 ± 1.38	1.54 ± 0.065	42.05	2.36 ± 0.23	0.993
SG/67-s-E	273.82 ± 22.66	2.16 ± 0.319	126.77	1.88 ± 0.23	0.976
SBA15/67	73.4 ± 3.92	2.14 ± 0.295	34.29	2.18 ± 0.62	0.965
SBA15/67-s-E	342.78 ± 9.21	1.53 ± 0.092	224.04	2.37 ± 0.33	0.987
SBA15/143	77.82 ± 2.39	1.57 ± 0.111	49.57	2.74 ± 0.48	0.979
SBA15/143-s-E	107.79 ± 3.32	1.61 ± 0.108	66.95	2.45 ± 0.39	0.983
Free CPO	522.97 ± 36.45	2.24 ± 0.27	234.47	2.03 ± 0.44	0.981
Silanized CPO	638.17 ± 17.46	1.64 ± 0.09	389.13	2.43 ± 0.30	0.988

Since enzyme molecules were randomly adsorbed on the surface of silica-based materials through physical adsorption, it is not surprising that they could present active site blockage or a change in its enzymatic conformation to inactive forms (*vide infra*). The similar catalytic turnovers should come preferentially from a bad orientation of CPO in the material surface since the difference in CPO load did not justify such variation. In fact, such phenomenon has already been described for immobilized HRP [31] and CPO [20] on different mesoporous materials. Another plausible explication is that the chemical nature of the material's surface modified the enzyme conformation to a less active one [32]. Since enzyme orientation and the nature of material's surface itself could influence enzymatic activity, we tested the same materials as supports but through covalent binding using APTEOSB as spacer arm.

The silica-based materials bearing a 67 Å pore size showed a notable enhancement in k_{cat} when compared to physical immobilization (see Table 2). The SBA15/67-s-E and SG/67-s-E showed a 4.7- and 4.2-time increase in k_{cat} when compared to their physical adsorption counterparts. Since CPO was covalently adsorbed on the surface of SG/67 and SBA15/67, it should be more accessible to substrate and bulk-medium oriented with minima mass transfer concerns as discussed elsewhere [33]. Moreover, the enzymatic activity might be enhanced through the hydrophobic environment produced by the organosilane modification as mentioned above.

Furthermore, the covalent approach in SBA15/143-s-E slightly enhanced the catalytic turnover (1.39 times) when compared with the physical adsorption. Such behavior relates to the larger pore size of the material embedding easily CPO with possible mass transfer concerns that could restrict flexible conformations of the enzyme [20] or block the entrance of the active site. Since the K_h values were very similar among all prepared materials and soluble enzymes, the catalytic efficiencies reflected mainly the catalytic turnover without significant limitations involving substrate affinity or mass transfer concerns. It is important to notice that the kinetic curves showed a sigmoidal profile with a *n* parameter from the Hill equation greater than one in all cases (Table 2). Such phenomenon was recently attributed to positive kinetic cooperativity on the oxidation of 4,6-DMDBT by free CPO [25].

Considering the oxidation of organosulfur compounds, the use of covalently immobilized CPO in the surface of SBA15/67 allowed the oxidation of 4,6-DMDBT (224.04 $\mu M^{-1}\,min^{-1}$) in miscible organic aqueous media at the same extent as the free enzyme (234.47 $\mu M^{-1}\,min^{-1}$). Since SG/67-s-E achieved a lower catalytic activity (126.77 $\mu M^{-1}\,min^{-1}$) that SBA15/67-s-E, the material should further possess an ordered structure, a higher surface area and a higher silanol/siloxane ratio.

3.4. Thermal residual activity and reusability of immobilized CPO on silica-based materials

A completely different scenario appeared in the thermal residual activity of free CPO, silanized-CPO, physical and covalent modified biocatalysts (Fig. 7). The former showed first a ther-

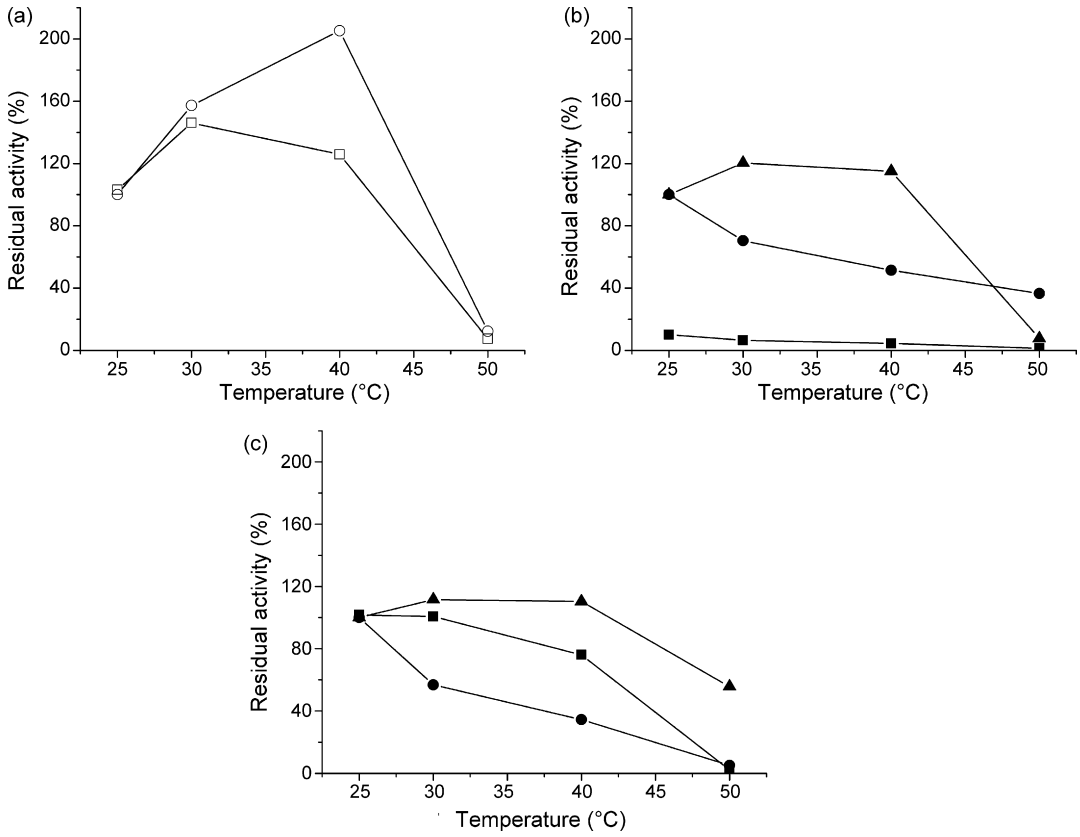

Fig. 7. Residual activity of (a) soluble enzymes, free-CPO (◯), and silanized CPO (s-E, □); (b) physical adsorbed CPO and (c) covalent immobilized CPO on SG/67 (●), SBA15/67 (■) and SBA15/143 (▲).

mal activation for the 4,6-DMBT oxidation (215%) between 25 and 40 °C followed by an important drop on residual activity at 50 °C. Here, it is evident that CPO suffered some changes with temperature in its protein conformation, which altered the catalytic activity as seen by the bathochromic shift of the main fluorescence peak (see supporting information). The diminution on residual activity was also observed on monochlorodimedone oxidation using CPO and was attributed to thermal reaction activation followed by the loss of activity [21]. Moreover, it was found that the activity loss with temperature was due to the release of the heme group from HRP [34].

The physical immobilized CPO showed the lowest thermal residual activity of all assays for 4,6-DMDBT oxidation. Possible sources of activity loss may occur through contact with material surface or due to changes in the microenvironment of the enzyme. Silica is a known catalyst for some oxidation reactions that could modify CPO structure with activity loss [32]. For example, cytochrome c showed less activity when it was directly immobilized on synthetic clay (laponite) than on organo-tailored clays [31]. It is believed that an organic spacer protects the enzyme against the chemical nature of the silica-based materials.

The s-E showed a similar picture with minor thermal activation because of the covalent bond with the APTEOSB spacer arm and the reduction of possible conformations that CPO can acquire. Moreover, covalent immobilized CPO for all materials retained the 100% initial activity of free CPO and s-E at 25 °C and showed the largest residual activity until 50 °C. The residual activity of SG/67-s-E and SBA15/67-s-E steadily decreased with temperature in accordance with free, silanized and physical immobilized CPO. Since CPO is mostly adsorbed here at material's surface without any pore protection, we presumed that CPO structure is somehow modified during its thermal incubation as seen by fluorescence spectra (see above), which provokes either enzyme denaturation or incapability to recognize 4,6-DMDBT as substrate. It is worth to note that covalent immobilization on larger pores than enzyme diameter did increase the residual activity of CPO, e.g. SBA15/143-s-E showed a 110% of residual activity at 40 °C while SBA15/67-s-E with a smaller pore size presented only 76%. Finally, the SBA15/143-s-E showed a thermal activation from 30 to 40 °C with a 56% of residual activity at 50 °C. It is well established that CPO is more susceptible to temperature than other peroxidases as HRP [20]. Nonetheless, we have achieved an important improvement in the residual activity of covalent immobilized CPO (SBA15/143-s-E) that differs from the mentioned work. Indeed, CPO was still capable for 4,6-DMDBT oxidation after incubation at 50 °C during 2 h. In contrast, Butler and coworkers reported a total activity loss using the MCD assay for CPO after incubation at 70 °C during 1 h [20].

Finally, we undertook five sequential reaction cycles with all tested biocatalysts in order to evaluate their potential reusability (Fig. 8). Concerning the physical immobilization, the SBA/143 material revealed the best residual activity after five reaction cycles. Indeed, it showed 44.6% of residual activity against 39 and 17% corresponding to SBA/67 and SG/67, respectively. It seems here that the larger pore size could effectively protect the protein against conformation changes to less active forms as well as maintain the enzyme inside the material with lesser leaching than the other materials.

On the other side, the CPO covalently attached to silica-based materials reached a higher residual activity after five reaction cycles than the physical approach. The ordered materials showed a 67.7% of residual activity against the 32% attained by the amorphous silica gel. In contrast, immobilized CPO on the surface of

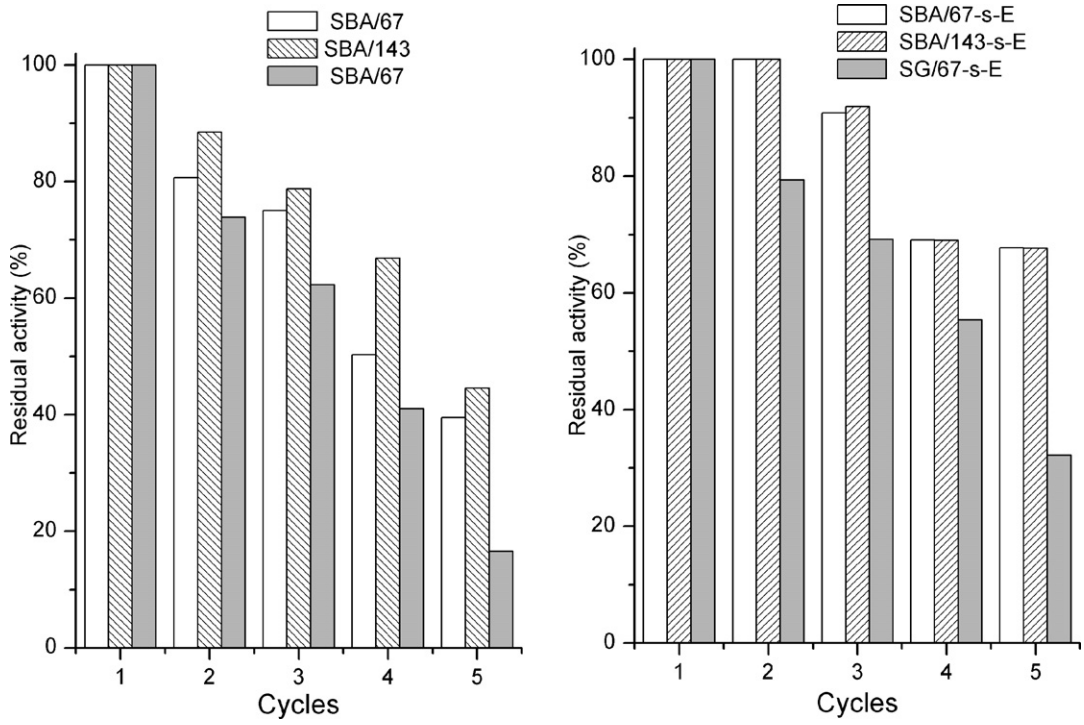

Fig. 8. Reusability of physical (left) and covalent (right) immobilized CPO on silica-based materials for 4,6-DMDBT oxidation.

glass beads showed a 30% of residual activity after five reaction cycles at pH 3 [23], which is similar to the results obtained for SG/67-s-E. The SBA materials showed similar residual activities throughout the cycles of reaction but higher values when compared to SG/67-s-E. It is clear that the presence of mesopores in addition with covalent immobilization protect the enzyme against denaturation and leaching.

4. Conclusions

In this work, we have shown that immobilized CPO on different silica-based materials catalyzes the oxidation of a recalcitrant and diesel-containing organosulfur compound (4,6-DMDBT). The use of silica-based materials as supports through the covalent approach with a high surface area as well as a high silanol/siloxane ratio enhanced the enzymatic activity, thermal stability and reusability of CPO. The covalent immobilized CPO in SBA15/143 showed the higher residual activity at 50 °C and reusability after five reaction cycles for 4,6-DMDBT oxidation.

Silica-based materials as SG/67 and SBA15/67 allowed a high physical adsorption capacity of CPO but the better results on catalytic efficiency, residual activity and reusability were obtained through a larger pore size in SBA15/143. The use of amorphous silica with no pores and low silanol/siloxane ratio for CPO immobilization resulted in biocatalysts with the poorer enzymatic load, catalytic efficiency, residual activity as well as reusability.

The oxidation of 4,6-DMDBT at 25 °C will be more efficient using any of the assayed SBA15 materials as covalent supports of CPO. Nevertheless, the SBA15/143-s-E should be preferred for 4,6-DMDBT oxidation when the reaction temperature is between 40 and 50 °C in the basis of its better performances. Further studies are needed in order to ascertain the type and role of the spacer arm, the silanol/siloxane ratio as well as the upper limit of pore size of supports in the catalytic efficiency and stability of immobilized CPO.

Acknowledgements

The authors thank the Mexican Petroleum Institute for financing support, Laboratorio de Caracterización Molecular (IMP) and Laboratorio de Fisicoquímica e Ingeniería de Proteínas (Faculty of Medicine, UNAM) for technical assistance. C.M. received a doctoral grant from IMP and CONACyT (Mexico).

Appendix A. Supplementary data

Supplementary data associated with this article can be found, in the online version, at doi:10.1016/j.molcatb.2007.06.012.

References

[1] B.J. Nablo, T.Y. Chen, M.H. Schoenfisch, J. Chem. Am. Sci. 23 (2001) 9712.
[2] M. Hartmann, Chem. Mater. 17 (2005) 4577.
[3] Y. Wang, F. Caruso, Chem. Mater. 17 (2005) 953.
[4] D. Enke, F. Janowski, W. Schwieger, Micropor. Mesopor. Mater. 60 (2003) 19.
[5] M.L. Ferrer, F. del Monte, D. Levy, Chem. Mater. 14 (2002) 3619.
[6] M. Hartmann, A. Vinu, Langmuir 18 (2002) 8010.
[7] A. Cauvel, G. Renard, D. Brunel, J. Org. Chem. 62 (1997) 749.
[8] E. Zhao, J. Feng, Q. Huo, N. Melosh, G.H. Fredrickson, B.F. Chmelka, G.D. Stucky, Science 279 (1998) 548.
[9] A. Vinu, V. Murugesan, O. Tangermann, M. Hartmann, Chem. Mater. 16 (2004) 3056.
[10] H.H.P. Yiu, C.H. Botting, N.P. Botting, P.A. Wright, Phys. Chem. Chem. Phys. 3 (2001) 2983.
[11] L. Whasmon-Kriel, V.L. Jimenez, K.J. Balkus Jr., J. Mol. Catal. B 10 (2000) 453.
[12] S. Colonna, N. Gaggero, L. Casella, G. Carrea, P. Pasta, Tetrahedron: Asymmetry 4 (1993) 1325.
[13] H. Fu, H. Kondo, Y. Ichikawa, G.C. Look, C.H. Wong, J. Org. Chem. 57 (1992) 7265.
[14] E. Kilijunen, L.T. Kanerva, J. Mol. Catal. B: Enzyme 9 (2000) 163.
[15] J.A. Thomas, D.R. Morris, L.P. Hager, J. Biol. Chem. 245 (1970) 3129.
[16] J.A. Thomas, D.R. Morris, L.P. Hager, J. Biol. Chem. 245 (1970) 3135.
[17] A. Zacks, D.R. Dodds, J. Am. Chem. Soc. 117 (1995) 10419.
[18] S. Aoun, M. Babouléne, Enzyme Microb. Technol. 23 (1998) 380.
[19] M. Andersson, B.K. Samra, H. Holmberg, P. Adlercreutz, Biocatal. Biotransform. 17 (1999) 293.
[20] Y. Han, T.J. Watson, G.D. Stucky, A. Butler, J. Mol. Catal B: Enzyme 17 (2002) 1.
[21] J. Aburto, M. Ayala, I. Bustos-Jaimes, C. Montiel, E. Terrés, J.M. Domínguez, E. Torres, Micropor. Mesopor. Mater. 83 (2005) 193.
[22] F. van de Velde, F. van Rantwijk, R.A. Sheldon, J. Mol. Catal. B. Enzyme 6 (1999) 453.
[23] T.A. Kadima, M.A. Pickard, Appl. Environ. Microbiol. 56 (1990) 3473.
[24] R. Vazquez-Duhalt, M.P. Bremauntz, E. Bárzana, R. Tinoco, Enzymatic oxidation process for desulfurization of fossil fuels, US Patent 6,461,859 (2002).
[25] E. Torres, J. Aburto, Arch. Biochem. Biophys. 437 (2005) 224.
[26] D.H. Everett, Pure Appl. Chem. 31 (1972) 578.
[27] J. Sun, J.A. Moulijn, K.C. Jansen, T. Maschmeyer, M.C. Coppens, Adv. Mater. 13 (2001) 327.
[28] M.H. Lim, A. Stein, Chem. Mater. 11 (1999) 3285.
[29] A. Sayari, S. Hamoudi, Chem. Mater. 13 (2001) 3151.
[30] J. Aburto, A. Mendez-Orozco, S. Le Borgne, Chem. Eng. Process. 43 (2004) 1587.
[31] H. Takahashi, B. Li, T. Sasaki, C. Miyasaki, T. Kajino, S. Inagaki, Chem. Mater. 12 (2000) 3301.
[32] K.A. Carrado, S.M. Macha, D.M. Tiede, Chem. Mater. 16 (2004) 2559.
[33] R.J. Barros, E. Wehtje, F.A.P. Garcia, P. Adlercreutz, Biocatal. Biotransf. 16 (1998) 67.
[34] M.L. Smith, J. Paul, P.I. Ohlsson, K. Hjortsberg, D.G. Paul, P. Natl. Acad. Sci. U.S.A. 88 (1991) 882.